Al-Azhar University Civil Engineering Research Magazine (CERM)
Vol. (44) No. (2) April. 2022

STEEL FIBER EFFECT ON HIGH STRENGTH CONCRETE BEAMS REINFORCED WITH GFRP BARS

Mohamed Hamdy Elnagar , Saeed Ahmed Hasanine[2], El-Sayed Abdel Raouf [3]

[1]Assistant teacher of Structural Engineering Department, Faculty of Engineering, Al-Azhar University, Cairo, Egypt.

[2] Professor of Structural Engineering Department, Faculty of Engineering, Al-Azhar University, Cairo, Egypt.

[3] Professor of Structural Engineering Department, Faculty of Engineering, Ain Shams University, Cairo, Egypt.

الملخص العربي :

أصبحت قضبان البوليمر المقوى بالألياف الزجاجية (GFRP) بديلا رائدا غير قابل للتآكل لحديد التسليح . يعتبر تسليح الكمرات الخرسانية عالية القوة بقضبان البوليمر المقوى بالألياف الزجاجية (GFRP) حلا فعالا لما تقابله قوة الخرسانة العالية مع قوة الشد العالية لقضبان GFRP. هذا النوع من التسليح يؤدي إلى استخدام اقل نسبة تسليح في القطاع الخرساني مما يقلل من مشاكل التشغيلية للخلطة الخرسانية إلا أنه قد يكون هذا الحل معيبا عن طريق زيادة هشاشة الكمرات الخرسانة لذا وللتغلب على هذا العيب يقترح استخدام بعض أنواع الألياف لزيادة ممطولية الكمرات الخرسانية.

في هذا البحث تم إجراء دراسة تجريبية لمعرفة جدوى استخدام أسياخ GFRP في HSCBs، وتأثير إضافة الألياف الفولاذية إلى هذه الكمرات على السعة التحميلية للكمرة، والجساءة الرأسية، وعرض اول شرخ مرئي ومقارنة النتائج بنتائج كمرات مسلحة بأسياخ من الصلب التقليدية. اشتملت الدراسة التجريبية على 16 كمرة خرسانية عالية المقاومة بمقاومين مختلفين من الخرسانة مصنفة الي: ست كمرات مسلحة بنسبة 0.75٪ من أسياخ الصلب ونسب متفاوتة من ألياف الصلب (0٪، 1٪، 1.50٪)، وست كمرات مسلحة بـ 0.75٪ من أسياخ GFRP ونسب متفاوتة من ألياف الصلب (0٪، 1٪، 1.50٪)، وأربعة كمرات مسلحة بنسب متفاوتة من أسياخ GFRP (0.50٪، 1.0٪، 1.26٪، 1.51٪) و1.0٪ من ألياف الصلب. أشارت النتائج إلى أن الحمل الأقصى للانهيار في HSCBs يزداد بشكل ملحوظ مع زيادة أسياخ GFRP وأن سلوك الكمرات الخرسانية المسلحة بـ GFRP كان مختلفا مع تغير قوة الخرسانة ونسبة GFRP عند تعرضها لحمل معين. أيضا، كان استبدال حديد التسليح بأسياخ GFRP يسرع من ظهور الشروخ الأولية ويزيد من حمل الانهيار في HSCBs. انخفضت الجساءة الرأسية لـ HSCBs المسلحة بأسياخ GFRP غير المحتوية على ألياف الفولاذ وHSCBs المحتوية على 1.0٪ من ألياف الفولاذ والمدعومة بأسياخ GFRP، حيث وصلت إلى حوالي 28.3٪ و37.7٪ من صلابة HSCBs المقواة بأسياخ فولاذية على التوالي. من خلال زيادة قوة الخرسانة بنسبة 22٪، يزداد حمل الانهيار بنسبة 10٪، و11٪، و7٪ من حمل انهيار كمرة التحكم في الكمرات المسلحة بأسياخ GFRP والتي تحتوي على حجم ألياف فولاذية بنسبة 0٪، 1.0٪، 1.50٪ على التوالي.

الكلمات المفتاحية: مقاومة عالية، البوليمر المقوى بالألياف الزجاجية، العناصر المحدودة، التآكل، شروخ، ألياف الحديد، كمرات مسلحة ,انسيز .

1 ABSTRACT

The search for a non-corrosion alternative for steel reinforcement is daily expanding, especially in construction exposed to chemical attacks such as carbonation in aggressive environmental conditions. Glass Fiber Reinforced Polymer (GFRP) bars has become a pioneering alternative. Therefore, reinforcement of high-strength concrete beams with GFRP bars is an effective solution since the high strength of concrete corresponds to the high tensile strength for GFRP bars. This reinforcement type leads to the use of a minimum reinforcement ratio that reduces workability problems. However, this solution may be defective because it increases the brittleness of the concrete beams. To overcome this problem, it is suggested to use some types of fiber to increase the ductility of the structural beams. In this research, an experimental was conducted to find out the feasibility of using GFRP bars in HSCBs, and the effect of adding steel fibers to these beams on load-capacity of beams, vertical stiffness, and comparing these results with those of the traditional steel bars reinforcement. The study included 16 high strength concrete beams with two different concrete strength; six beams reinforced with 0.75% of steel bars and varying ratios of steel fibers (0% ,1% ,1.50%), six beams reinforced with 0.75% of GFRP bars and varying ratios of steel fibers (0% ,1% ,1.50%), and four beams reinforced with varying ratios GFRP bars (0.50%, 1.0%, 1.26%, and 1.51%) and 1.0% of steel fibers.

The results indicated that the maximum failure load of the HSCBs significantly increases with the increase of the GFRP bars more than 0.5% and the behavior in GFRP-reinforced concrete beams was different with the change of concrete strength and GFRP ratio when subjected to a given load. Also, it was revealed that the replacement of steel reinforcement with GFRP bars accelerates the appearance of the initial cracks and increases the failure load in HSCBs. The vertical stiffness for the HSCBs reinforced with GFRP bars decreased as it reached about 28.3% of the stiffness of the HSCBs reinforced with steel bars. By increasing concrete strength by 22%, the failure load increases by 10%, 11%, and 7% of control beam failure load in beams reinforced with GFRP bars and containing steel fiber volume by 0%, 1.0%, and 1.50% respectively.

Keywords: High Strength, GFRP, FEA, Corrosion, Cracks, Concrete Beam, ANSYS, Steel Fiber.

1. INTRODUCTION

High-strength concrete was applied in many structures in the past few years. To get concrete of high strength, various materials have been added, that have superior durable properties. It is known that concrete is a brittle material, therefore a sudden failure may occur in the various concrete members that may lead to catastrophic damage to the structure and the people living in these structures. Also, concrete shrinkage and volume reduction happen due to the loss of moisture, which results in cracks and more concrete deformation [1] [2] .

So, due to the fiber high strength, energy absorption capacity, and strain-hardening behavior with multiple micro-cracks, the use of various fibers in the concrete has many advantages such as acting as crack arresters, decreasing the propagation of cracks, increasing the ductility of the structural members, improving concrete brittle behavior, reducing permeability, increasing toughness for concrete members, resistance to crack growth and increasing the flexural capacity of the structural members [3].

Most of the conventional fiber-reinforced cementitious materials involve the use of single fiber types with different sizes. The individual fiber reinforcement method is effective in a range of strain and cracks opening and improved strength or ductility. Some studies have shown that hybrid fiber-reinforced concrete (HFRC) can improve the bond between FRP bars and concrete [4] [1]. Steel fibers appear to have a better performance in flexural strength unlike other fiber types [5]. Therefore, research has increased recently, which studied the effect of the weight percentages, size, and shape of steel fibers and being single or hybrid with other fibers on the behavior and properties of concrete, especially high-strength concrete, because it is more brittle. It was found that the addition of steel fiber increases the compressive strength by 16%, 20%, and 3% at the age of 3, 7, and 28 days respectively, increases the flexural toughness index up to 7.7 times [6],[5]. Also, It was found the use of steel fibers with a high aspect ratio increases tensile strength , improves impact resistance, and reduces workability and crack expansion [7]. Yoo and Banthia found that the use of twisted steel fibers in ultra high-performance fiber-reinforced concrete **(**UHPFRC) increases the tensile strength, strain capacity, and flexural strength by about 32%, 205%, and 167% respectively compared to short straight steel fibers. [8]. Jadidi et al. found that combining two types of steel fibers (hooked and crimped) have aspect ratios of 30 and 50 with different weight percentages (1.5%, 2%, and 2.5%) caused a considerable increase in concrete bending strength compared to fibreless concrete and single fiber concrete [9]. Yuan et al. investigated the effect of hybrid combinations of polyethylene (PE) fiber and steel fiber (SF) using a fiber volume fraction of 0.0 and 1.5% on no-slump high-strength concrete (NSHSC). Specimens with a hybrid of SF and short PE fibers exhibited a higher compressive and flexural strength, flexural toughness, and energy dissipation capacity [1].

Karimipour et al., found that the steel fibers concrete that contains rubber waste increased shrinkage deformation with the increased rubber waste content, and used 2% SF with 5% rubber tire waste increased the flexural strength of the specimens by 23% [10]. Jin et al. found that steel fibers in high-performance concrete under the influence of static loads increased the ductility, hardness, tensile strength, and decreased the ratio between the prism and cube compression when increasing the proportion of steel fibers [11]. Qureshi et al. investigated the properties of high-strength concrete by adding steel fibers. Test results revealed adding steel fibers increases tensile strength in a linear manner with the increase rate higher in the first 7 days [12]. Z. Li et al. found that a 1.0% steel fiber volume ratio in high-strength concrete beams reinforced with BFRP bars under repeated loading increased the beam service load, decreased deflection by 59.36%, and improved the beam ductility by 17% [13]. Song and Hwang investigated the mechanical properties of high-strength steel fiber-reinforced concrete. The compressive strength of the concrete reinforced with 1.0% steel fiber improved by over 11.8% of the HSC [14]. Yang et al, (2016) studied ultimate loads, crack propagation behavior, load-deflection curves, and the damage to beams observed at the failure stage for concrete beams reinforced both with GFRP and steel bars. It was observed that the energy dissipation in GFRP-reinforced concrete beams was different from those of steel-reinforced concrete beams when subjected to a given load [15]. Gribniak et al. investigated the effect of the arrangement of GFRP tensile reinforcement on the flexural stiffness and cracking of concrete beams. It was found that the maximum crack opening was not necessarily adjacent to the maximum distance between cracks, with increasing reinforcement layers increases the flexural stiffness, and no relationship between crack widths and the crack spacing when the reinforcement layout changed (single or three layers) [16]. Qin et al. [64] aimed to increase the stiffness and flexibility of the concrete beams at the same time by combining steel bars with FRP in reinforcement. It was found that the best ratio of A_f /A_s in over-reinforced beam design had a range of 1 to 2.5 to provide enough post-elastic strength and stiffness [17] . El-Nemr et al. investigated the flexural behavior and serviceability performance of concrete beams reinforced with different types of GFRP bars whose surface profile was sand-coated and grooved. It was noticed that the cracking behavior tends to confirm that sand-coating of GFRP bars enhances the bond performance in concrete more than the helically grooved profile [18] .Ashour et al. tested twenty-seven reinforced high-strength concrete beams to study the effects of longitudinal tensile reinforcement ratio of steel, steel fiber content, and compressive strength on flexural behavior of reinforced concrete beams. It was noticed that tensile reinforcement ratio did not affect the additional moment strength that was provided by fibers. Also, when the concrete compressive strength and steel fiber content increased, the flexural rigidity increased significantly [19].

The previous presentation finds shortcomings in studying the effect of GFRP reinforcement ratios on behavior concrete beams, especially high strength, the advantages of adding steel fiber to the beams, and how their lower vertical stiffness increases.

2 LABORATORY EXPERIMENTS

2.1 GENERAL

The experimental work conducted in this project investigated the behavior of high-strength concrete beams reinforced with GFRP bars under flexural loading patterns. The parameters studied in these tests were the concrete strength, the ratio and type of longitudinal reinforcement, and steel fiber volume.

Sixteen beams were cast as shown in Table 1. The beams were divided into five groups.

Group (1) consisted of three beams and studied the effect of various volumes of steel fiber (0%, 1%, and 1.50%) on HSCBs reinforced with longitudinal steel bars by 0.75% under flexure loads, and the concrete mix (1) was used to cast these beams. Group (2) consisted of three beams and studied the effect of various volumes of steel fiber (0%, 1%, and 1.50%) on HSCBs reinforced with longitudinal steel bars by 0.75% under flexure loads, and the concrete mix (2) was used to cast these beams. Group (3) consisted of three beams and studied the effect of various volumes of steel fiber (0%, 1%, and 1.50%) on HSCBs reinforced with longitudinal GFRP bars by 0.75% under flexure loads, and the concrete mix (1) was used to cast these beams.

Group (4) consisted of three beams and studied the effect of various volumes of steel fiber (0%, 1%, and 1.50%) on HSCBs reinforced with longitudinal GFRP bars by 0.75% under flexure loads, and the concrete mix (2) was used to cast these beams.

Group (5) consisted of five beams and studied the effect of various ratios of longitudinal GFRP bars on HSCBs that contained 1% of fiber steel, and mix (2) was used to cast these beams.

2.2 BEAMS DETAILS

The RC beams with over all dimensions of 125 mm width, 250 mm depth and 2000mm length were tested. The beams were simply supported with a clear span of 1800mm.

The bottom longitudinal reinforcement with a diameter of 10mm was 3 steel bars for beams coded 3S10, 3S11, 3S15, 3S20, 3S21, and 3S25, 3 GFRP bars for beams coded 3G10, 3G11, 3G15, 3G20, 3G21, and 3G25, 2 GFRP bars for the 2G21 beam, 4 GFRP bars for the 4G21 beam, 5 GFRP bars the 5G21 beam, and 6 GFRP bars for the 6G2 beam as shown in Table 1.

The top reinforcement was 2 steel bars with a diameter of 10mm for all beams. It used the steel bars in the top beam in compliance with the recommendations of ECP 208-2005 [20].

The stirrups were 8mm diameter steel bars at 100mm spacing to avoid shear failure of the beams as shown in Fig. 1 and Fig. 2.

Table 1: Classification of Beams

Group No.	Beam No.	Beam Code	Mix No.	Fcu (MPa)	Steel Fiber Volume %	Bottom Rein. Type	Bottom Rein. ratio
Group (1)	1	3S10	Mix1	59.7	0	Steel	0.75%
	2	3S11		64.5	1		
	3	3S15		68	1.5		
Group (2)	4	3S20	Mix2	73	0	Steel	0.75%
	5	3S21		78	1		
	6	3S25		87.8	1.5		
Group (3)	7	3G10	Mix1	59.7	0	GFRP	0.75%
	8	3G11		64.5	1		
	9	3G15		68	1.5		
Group (4)	10	3G20	Mix2	73	0	GFRP	0.75%
	11	3G21		78	1		
	12	3G25		87.8	1.5		
Group (5)	13	2G21	Mix2	78	1	GFRP	0.50%
	11	3G21		78			0.75%
	14	4G21		78			1.01%
	15	5G21		78			1.26%
	16	6G21		78			1.51%

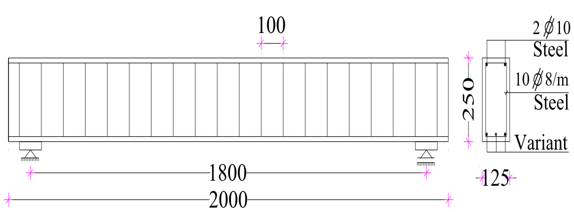

Fig. 1: Dimensions and reinforcement details


Fig. 2: Reinforcement for beam

2.3 FABRICATION OF TEST SPECIMENS

The beams were fabricated at the Concrete Laboratory of the Civil engineering Department, Faculty of Engineering, Al-Azhar University. The reinforced concrete specimens were fabricated where reinforcement cages were prepared, then the formwork was made of thick plywood, and then GFRP bars reinforcement was installed in the formwork. Then, concrete was cast with a target cube compressive strength of 60MPa. The concrete was compacted after casting using an electrical vibrator for three minutes. The curing of specimens with water was started 24 hours after casting, as shown in Fig. 3.

Fig. 3: Casting and curing

2.4 MATERIAL PROPERTIES

The test beams used in this program were made from local material except GRFP bars. Two diverse types of coarse aggregate were used in this study: dolomite and basalt. The coarse aggregates for the first and second mix were composed of crushed dolomite and crushed basalt respectively with a size ranging from 0.75 to 25.0 mm. The batches used were all the good quality with uniform characteristics and free from injurious materials. The partial shape was a combination of round and sub-angular. Apparent specific gravity for dolomite and basalt was 2.65 and 2.75, respectively. Moreover, Fine aggregate used was composed of the sand siliceous material. It was clean and free from injurious and organic materials. Torah Portland cement CEMI 52.5 N was used in the experimental work, which conforms to the Egyptian standard specification (ES 4756/1-2007) for Portland cement [21]. As for the water used in all mixes, it was clean drinking fresh water free from impurities. The value of water/cement ratio used was chosen based on the total weight of water added to air dry materials. Two diverse types of steel were used in this study; one of them was normal mild steel with yield strength 240MPa, and the other was high tensile steel with yield strength (proof strength) 400MPa. The normal mild steel bars were round, smooth and with diameter of 8mm that were used as stirrups. The high tensile steel bars were round, not smooth, and with diameters of 10 and were used for the top reinforcement. The mechanical characteristics of high tensile steel, as reported by manufacturer are presented in).

Fig. 4: GFRP bars

Fig. 5: Hooked steel fiber

Table 2. The GFRP bars used in the experimental study were straight shaped as shown in Fig. 4. Such bars were tested in the National Research Centre of Egypt. Tensile tests were carried out on three specimens of the bars. The results of ultimate strength, strain, and elastic modulus are listed in

Table 3. The steel fiber used in this study was hooked end type with an aspect ratio of (L/D) 43.75 as shown in Fig. 5. The basic dimensions of this fiber were 35×0.8 mm with 45° hooked ends which are generally considered too slow to deform during pull-out from concrete ensuring a controlled ductile failure. However, it must be noted that adding a large amount of relatively long and stiff steel fibers into concrete may cause workability problems. The fiber content of 78.5 kg/m3 adopted is corresponded to 1.0% by volume of the concrete matrix for the specimen (3G11).

Fig. 4: GFRP bars

Fig. 5: Hooked steel fiber

Table 2. Mechanical characteristics of high tensile steel

Steel Properties	
Proof strength “ƒy” (MPa)	400
Ultimate Strength “ƒu” (MPa)	520
Young’s Modulus “E” (MPa)	200,000
Yield Strain “εy”	0.002
Strain at Maximum load “εy”	0.008
Maximum Strain “εy”	0.016

Table 3. Mechanical characteristics of GFRP bars

Properties of GFRP bars	Sample No.		
	1	2	3
Nominal Diameter (mm)	10		
Nominal Area (mm2)	78.57		
Mass per Meter Run (gm/mm)	138		
Ultimate Load (KN)	85.5	77.84	80.72
Ultimate Tensile strength (MPa)	1088	990.71	1027.3
Max. Strain	N.M	0.0229	0.0258
Modulus of Elasticity (MPa)	N.M	43262	39820

2.5 CONCRETE MIX

A study was carried out to obtain the controlled concrete mix (Mix1) which used dolomite as coarse aggregate with no steel fiber in order to reach the required compressive strength (60Mpa). Six mixes were designed with different coarse aggregate types and different steel fiber volumes which led to different concrete strength. Mixes proportioning of concrete are presented in

Table 4.

Table 4 Proportioning of concrete mixes

Mix No.	Steel Fiber (kg)	Coarse Aggregate Type	Cement (kg)	Coarse Aggregate (kg)	Fine Aggregate (kg)	Water (kg)	Silica Fume (kg)	Superplasticizer (kg)
Mix (1)	0	Dolomite	500	970	780	185	25	12.5
	78.5							
	117.75							
Mix (2)	0	Basalt	500	1180	540	168	40	14
	78.5							
	117.75							

2.6 SPECIMENS PREPARATION AND TEST SET-UP

Three standard cubes, 150x150x150 mm, were taken from each the concrete mix during the casting of each specimen. Results of the cubes tests after 28 days are presented in Table 5. Instrumentation of specimens included three Linear Variable Displacement Transducers (LVDT) were used for measuring deflection at three points, strain gauges were used for reinforcement bars at the mid-bar, strain gauges were used for concrete at top mid-span, and a load cell to measure the load of the testing machine as shown Fig. 6. The tests were carried out under a controlled load of four-point loading up to failure using a manual hydraulic jack of 1000 KN capacity as shown in Fig. 7. The load increment was constant for beams specimens at 5kN. Two concentrated loads at 300mm from the mid span were applied on the beam using a distributing steel I-beam, supported on two steel rods and rested on neoprene pads. During testing, the loading was paused at different load levels to visually inspect the beam. Crack propagation was visually observed, and the cracks were marked on the surface of the tested specimen.

Table 5. Compression test results on standard cubes

Mix No.	Cubes	Steel fiber Volume %	F_{cu} (MPa)
Mix1	Mix 10	0.00 %	59.7
	Mix 11	1.00 %	64.5
	Mix 15	1.50 %	68
Mix2	Mix 20	0.00 %	73
	Mix 21	1.00 %	78
	Mix 25	1.50 %	87.8

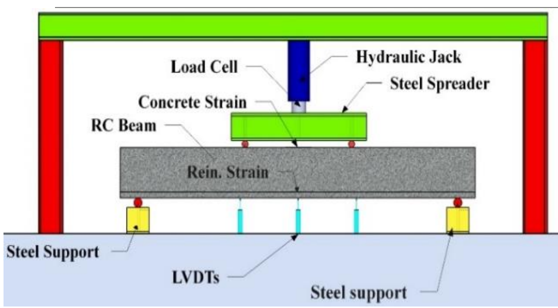

Fig. 6 :Instrumentation used

Fig. 7 :Test set up and load pattern

3 RESULTS OF EXPERIMENTAL STUDY

The failure loads, maximum measured vertical deflection at mid span, maximum top concrete compression strain, maximum bottom longitudinal reinforcement strain and vertical stiffness at 80 % of failure load for control beam (3S10) are summarized in

Table 6

Table 6. Results of the experimental beams

Group No.	Beam Code	SFV (%)	Mix No.	F_{cu} (MPa)	P_u (kN)	Δ_u (mm)	ε_{Cmax}	ε_{Rmax}	Stiffness @ 80% P_{cf} (kN/mm)
G1	3S10	0	1	59.7	99.5	19.5	-0.001461	0.005287	12.24
	3S11	1		64.5	132.6	17.4	-0.001737	0.019676	16.82
	3S15	1.5		68	156.1	18.9	-0.000432	0.019676	18.50
G2	3S20	0	2	73	112.4	20.2	-0.003067	0.019676	12.34
	3S21	1		78	128.1	21.8	-0.003096	0.019676	14.33
	3S25	1.5		87.2	148.7	26.8	-0.000579	0.018229	21.54
G3	3G10	0	1	59.7	130.5	35.3	-0.001740	0.019562	3.69
	3G11	1		64.5	149.5	27.5	-0.003016	0.016997	5.14
	3G15	1.5		68	183.4	37.0	-0.001735	0.017812	6.28
G4	3G20	0	2	73	144.4	33.2	-0.002472	0.013723	4.84
	3G21	1		78	166.8	35.9	-0.001488	0.027413	7.72
	3G25	1.5		87.2	197.3	40.5	-0.001932	0.022572	6.52
G5	2G21	1	2	78	143.3	30.9	-0.001604	0.019675	5.41
	3G21	1		78	166.8	35.9	-0.001488	0.027413	7.72
	4G21	1		78	201.0	36.8	0.01903	-0.001931	8.00
	5G21	1		78	231.2	37.7	-0.002399	0.015521	9.41
	6G21	1		78	277.5	43.6	-0.001365	0.013039	10.32

3.1.1 EFFECT OF STEEL FIBER VOLUME ON HSCBS REINFORCED WITH STEEL BARS.

3.1.1.1 FAILURE LOAD

From Fig. 8, Fig. 9, and

It is noted that the increase of steel fiber volume in concrete beams induces an increase in failure load. The failure load of the 3S11 and 3S15 beams was higher than the 3S10 beam by 33 % and 57% respectively. The failure load of the 3S21 and 3S25 beams was higher than the 3S20 beam by 14 % and 32% respectively. It is noted that by increasing concrete strength by 22%, the failure load increases by 13% for the beams containing no steel fiber. For beams that contain steel fiber by 1 and 1.5 %, the load failure decreased by 3% and 4% respectively.

It is noted that the steel-reinforced concrete beam failed due to yielding in steel bars then crushing in concrete occurred and the typical load-deflection behavior of beams was linear up to yield load, when the yield of the longitudinal steel reinforcement was reached; the behavior changed to be nonlinear up to failure.

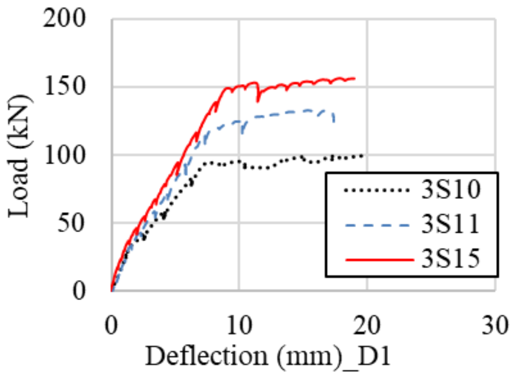

Fig. 8 :Load –deflection at mid-span relationship for group (1)

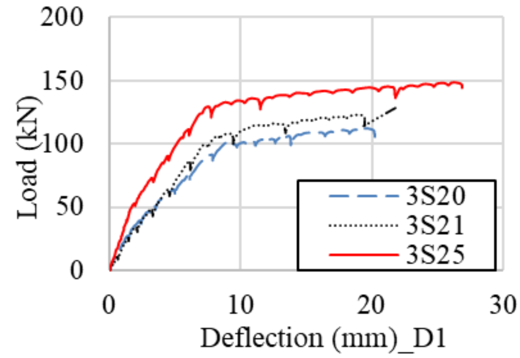

Fig. 9 :Load –deflection at mid-span relationship for group (2)

3.1.1.2 VERTICAL STIFFNESS

Fig. 10, Fig. 11, and show the relationship between the vertical stiffness and the vertical load at mid-span for the group (1) and group (2).

As the vertical load increased, the stiffness started to decrease for all beams. However, the rate of decrease in the stiffness of the 3S11 beam and 3S15 beam was less than the 3S10 beam. Also, the rate of decrease in the stiffness of the 3S21 beam and 3S25 beam was less than the 3S20 beam.

The vertical stiffness deterioration goes through three stages for each beam, although its value varies. The first stage is from the no-loaded to the stable loading mode. The second stage after stable loading occurred where the stiffness deterioration is rather weak as indicated by the semi-horizontal line. This stage is generally representative of the beam stiffness. The third stage before the beam failure: rapid breakdown of the stiffness occurred. This stage started at a different value of each beam where it started for 3S10 and 3S11 beams earlier than the 3S15 beam.

At a given load of 80 kN,

Table 6 shows that the stiffness for 3S11 and 3S15 was higher than 3S10 by 31% and 44.4% respectively due to steel fiber. As the concrete strength increases, the deterioration of stiffness was lower. At a load of 80 kN, the stiffness for 3S20,3S21 and 3S25 was higher than 3S10 by 0.08 %, 17 %, and 75.9 % respectively.

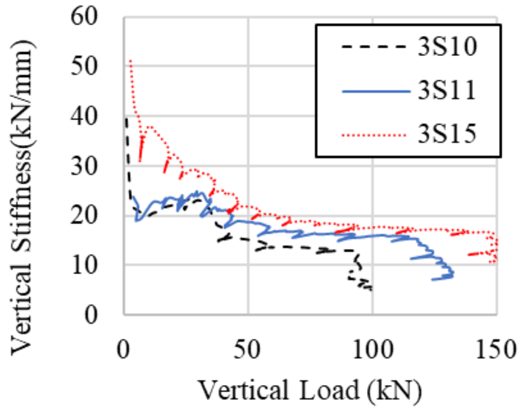

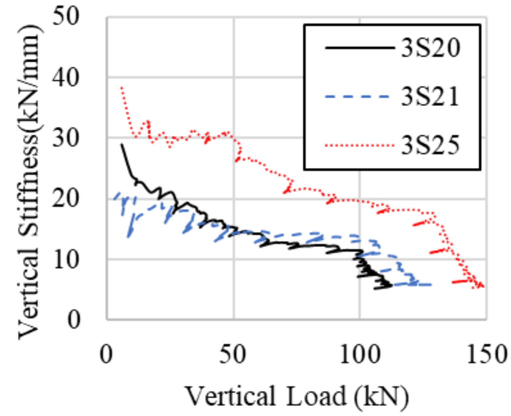

Fig. 10: Vertical stiffness- vertical load relationship for group (1)

Fig. 11 :Vertical stiffness- vertical load relationship for group (2)

3.1.2EFFECT OF STEEL FIBER VOLUME ON HSCBS REINFORCED WITH GFRP BARS

3.1.2.1 FAILURE LOAD

From Fig. 12, Fig. 13 and

Table 6; It is noted that the increase of steel fiber volume in concrete beams induces an increase in failure load. For group (3), The failure load of the 3G11 and 3G15 beams was higher than the 3G10 beam by 15 % and 41% respectively. For group (4), The failure load of the 3G21 and 3G25 beams was higher than the 3G20 beam by 16 % and 37% respectively.

It is noted that by increasing concrete strength by 22%, the failure load increases by 10%, 11%, and 7% in beams that contain steel fiber volume by 0%, 1.0%, and 1.50% respectively. It is noted that the failure of beams was due to crushing in concrete occurred then rupture in GFRP bars. The typical load-deflection behavior of beams was linear up to failure. When the concrete was cracked, the linear slope decreased which refers to the transfer of all stresses to GFRP bars.

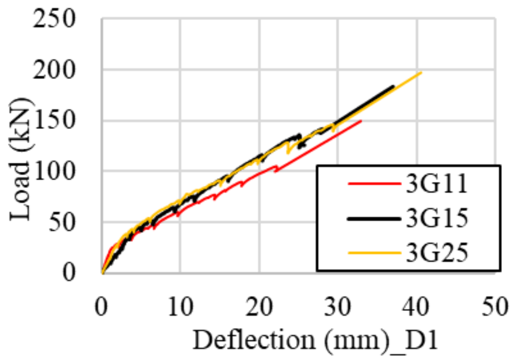

Fig. 12 :Load –deflection at mid-span relationship for group (3)

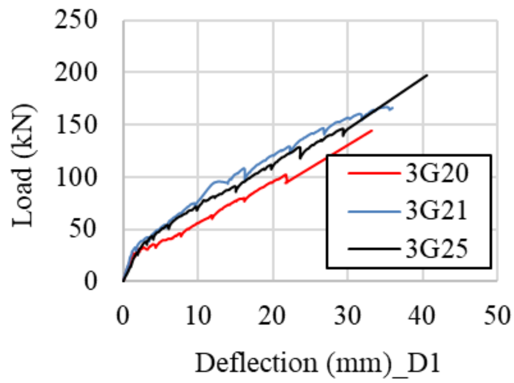

Fig. 13 :Load –deflection at mid-span relationship for group (4)

3.1.2.2 VERTICAL STIFFNESS

Fig. 14 and Fig. 15 show the relationship between the vertical stiffness and the vertical load at mid-span for group (3) and (4).

As the vertical load increased, the stiffness started to decrease for all beams. However, the rate of decrease in the stiffness of 3G11 beam and 3G15 beam was less than the 3G10 beam. Also, the rate of decrease in the stiffness of the 3G21 and 3G25 beams was less than 3G20 beam.

The vertical stiffness deterioration goes through three stages for each beam, although its value varies. The first stage is from the no-loaded to the stable loading mode. The second stage is before the concrete cracked occurred; where the stiffness deteriorated is significantly. The third stage is after the concrete cracked to beam failure where the stiffness deterioration weakly as indicated by the semi-horizontal line. This stage is generally representative of the beam stiffness.

At a given load of 80 kN, the stiffness for 3G11 and 3G15 was higher than 3G10 by 39% and 70% respectively and the stiffness for 3G20, 3G21, and 3G25 was higher than 3G20 by 31%, 109% and 76% respectively due to steel fiber. As the concrete strength increases, shows that the deterioration of stiffness was lower.

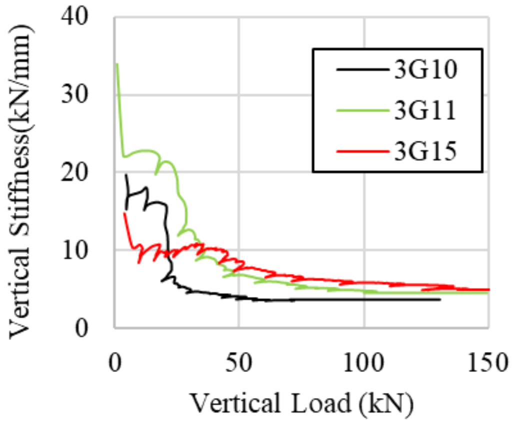

Fig. 14 :Vertical stiffness- vertical load relationship for group (3)

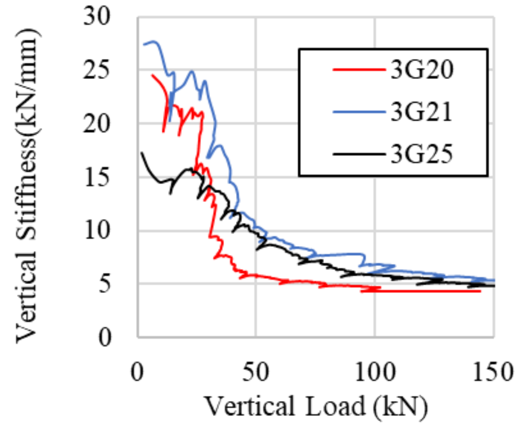

Fig. 15 :Vertical stiffness- vertical load relationship for group (4)

3.1.3EFFECT OF GFRP RATIO VARIATION ON HSCBS REINFORCED WITH STEEL FIBER BY 1%

3.1.3.1 FAILURE LOAD

Fig. 16 compares load-deflection relations of the group (5). It is noted that the increase of GFRP ratio induces an increase in failure load.

The failure load of beams 3G21, 4G21, 5G21, and 6G21 was 15 % and 16%,40%, 61%, and 94% higher than 2G21 respectively. It is noted that with the increase in the GFRP bars, the beam will be more able to resist loads. This will lead to a delay in the failure of the beam.

3.1.3.2 VERTICAL STIFFNESS

Fig. 17 shows the relationship between the vertical stiffness and the load at mid-span for the group (5).

As the vertical load increased, the stiffness started to decrease for all beams. However, the rate of decrease in the stiffness with an increase of GFRP bars ratio was lower.

The stiffness for the 3G21,4G21, 5G21, and 6G21 beams was higher than 2G21 by 16%, 40%, 61%,and94%respectively.

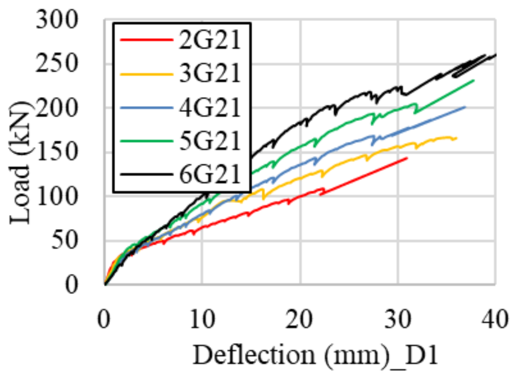

Fig. 16 :Load –deflection at mid-span relationship for group (5)

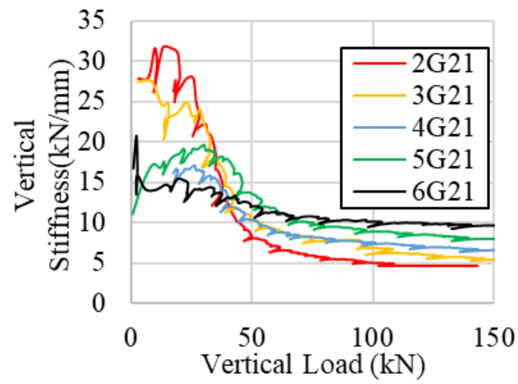

Fig. 17 :Vertical stiffness- vertical load relationship for group (5)

3.1.4 EFFECT OF TYPE LONGITUDINAL REINFORCEMENT ON HSCBS

To study the effect of type longitudinal reinforcement on HSCBs, some previous beams will be studied. Each beam will be compared with its counterpart in reinforcement ratio, steel fiber volume, and concrete strength. A new group was created named (group 6); where the 3S10, 3S11, 3S15, 3S20, 3S21, and 3S25 beams reinforced with steel bars are corresponding to the 3G10, 3G11, 3G15, 3G20, 3G21, and 3G25 beams reinforced with GFRP bars respectively.

3.1.4.1 FAILURE LOAD AND VERTICAL STIFFNESS

Fig. 18 shows the rate of load increase and the rate of stiffness decrease for group (6).

It is noted that the failure load increased as a result of replacing the steel with GFRP bars. on another hand, the vertical stiffness decreased significantly.

The failure load of the 3G10, 3G11, 3G15, 3G20, 3G21, and 3G25 beams was 31%,13%,18%,28%, 30%, and 33% higher than the 3S10, 3S11, 3S15, 3S20, 3S21, and 3S25 beams respectively.

In contrast, the vertical stiffness of the 3G10, 3G11, 3G15, 3G20, 3G21, and 3G25 beams was 70%,69%, 66% ,61%, 46%, and 70% lower than the 3S10, 3S11, 3S15, 3S20, 3S21, and 3S25 beams respectively due to the high elastic modulus of steel versus GFRP bars, which reach 5 times of it.

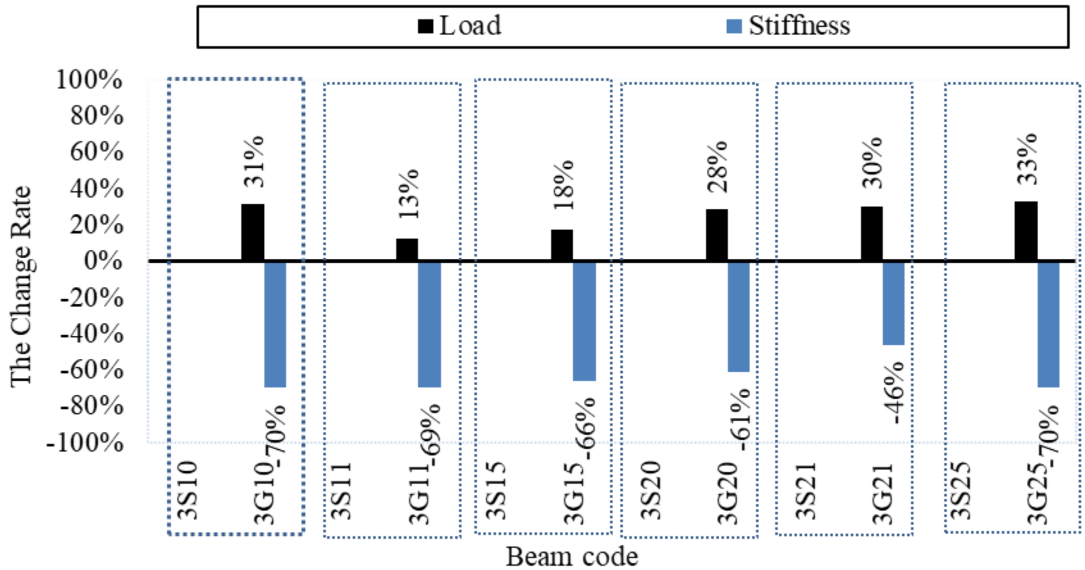

Fig. 18 :Load and stiffness change rate for Group (6)

3.1.5 EFFECT OF ALL PARAMETERS STUDIED ON HSCBS

3.1.5.1 FAILURE LOAD

By comparing failure load for each beam with the failure load for the control beam in Fig. 19, the following was observed:

1. By increasing concrete strength by 22%, the failure load increased by 13% for the beams reinforced with steel bars and not containing steel fiber;
2. Maximum failure load reached 179 % when the ratio of GFRP bars reinforcement doubled, and steel fiber volume was by 1%;
3. To double the failure load, steel was replaced with GFRP bars, and the highest concrete strength and highest steel fiber were used;
4. Approximately 0.25% of GFRP bars is equivalent to 0.5% of steel fibers volume.

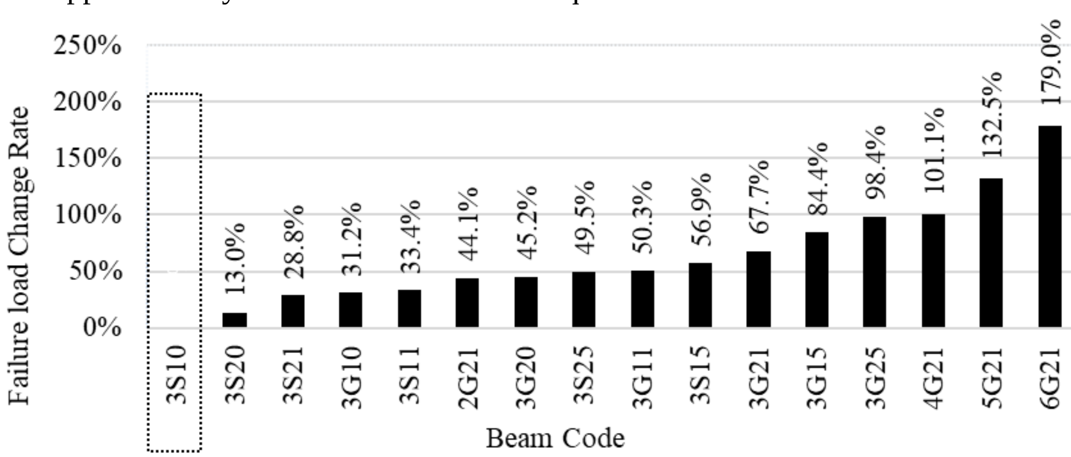

Fig. 19 :Failure load change rate for beams

3.1.5.2 VERTICAL STIFFNESS

By comparing vertical stiffness for each beam with the vertical stiffness for the control beam when 80% of failure load of control beam in Fig. 20, the following was observed;

1. All beams reinforced with GFRP are less stiff than the control beam reinforced with steel;
2. When the concrete strength was increased or steel fiber was added, the stiffness of the beams reinforced with steel is higher than the stiffness of the control beam;
3. Adding lowest amount of steel fiber in the beams was better than increasing concrete strength;
4. By doubling the GFRP bars ratio, the stiffness improved by 22%;
5. The vertical stiffness deteriorated by 70 % when replacing steel with GFRP bars.

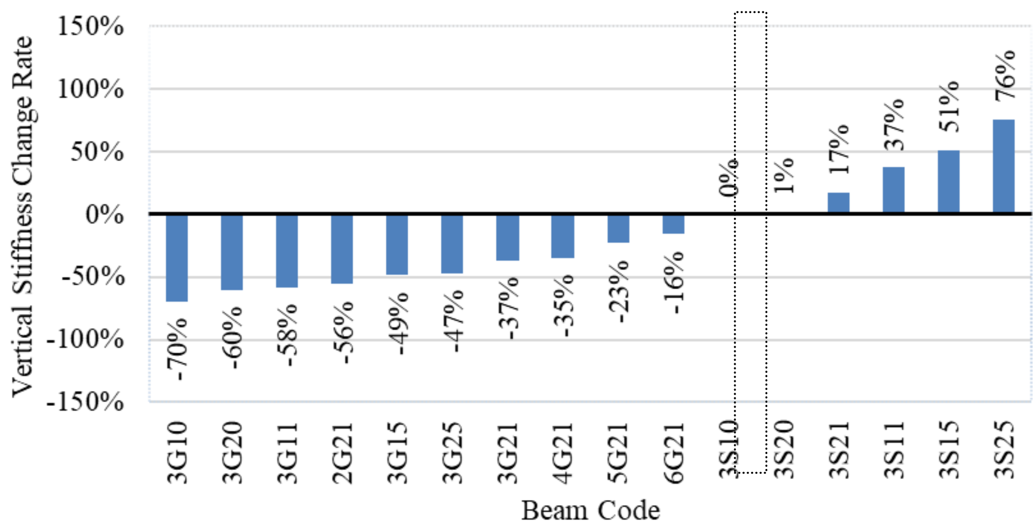

Fig. 20 :Beams Stiffness

3.1.5.3 EFFECT OF STEEL FIBER ON CONCRETE STRENGTH

The steel fiber in concrete increase in strength concrete, but the increasing is not large. Table 5 shows the effect of steel fiber volume on concrete strength. It is noted in Mix1 that the concrete strength increased by 8% and 14% when the steel fiber was 1 % and 1.50% respectively. Also, it is noted in Mix2 that the concrete strength increased by 7% and 20% when the steel fiber was 1 % and 1.50% respectively.

4 SUMMARY AND CONCLUSIONS

4.1 SUMMARY

In this research, the behavior of HSCBs reinforced with GFRP bars subjected to flexure loads was studied using an experimental study. An experimental study was conducted to study the effect of type and ratio of reinforcement, and the steel fibers volume on HSCBs.

4.2 CONCLUSIONS

i. The behavior of GFRP-reinforced concrete beams was different from the change of strength concrete and GFRP ratio when subjected to a given load;
ii. The vertical stiffness for the HSCBs reinforced with GFRP bars and the HSCBs containing 1.0 % of steel fiber reinforced with GFRP bars reached about 28.3% and 37.7% of the stiffness for the HSCBs reinforced steel bars respectively;
iii. The addition of steel fibers by 1% increases the concrete strength by 9.8 % and the vertical stiffness of the HSCBs reinforced with GFRB bars by 33%;
iv. The HSC corresponds to the high tensile strength for GFRP bars. Thus, the use of GFRP bars in HSCBs has physical significance as the entire concrete section exposed to flexure bending load, is used;
v. By increasing concrete strength by 22%, the failure load increased by 13% for the beams reinforced with steel bars and not containing steel fiber;
vi. By increasing concrete strength by 22%, the failure load increased by 10%, 11%, and 7% of control beam failure load in beams reinforced with GFRP bars and containing steel fiber volume by 0%, 1.0%, and 1.50% respectively;
vii. Replacing steel with GFRP bars makes the failure brittle;
viii. Maximum failure load reached 179 % when the ratio of GFRP bars reinforcement doubled, and steel fiber was by 1%;
ix. To double the failure load, steel was replaced with GFRP bars, and the highest concrete strength and highest steel fiber were used;
x. For failure load, approximately 0.25% of GFRP bars is equivalent to 0.5% of steel fibers.
xi. All beams reinforced with GFRP are less stiff than the control beam reinforced with steel;
xii. When the concrete strength was increased or steel fiber was added, the stiffness of the beams reinforced with steel is higher than the stiffness of the control beam;
xiii. For vertical stiffness, adding lowest amount of steel fiber in the beams was better than increasing concrete strength;
xiv. By doubling the GFRP bars ratio, the stiffness improved by 22%;
xv. The vertical stiffness deteriorated by 70 % when replacing steel with GFRP bars;
xvi. The spread of cracks and their widening in the beams reinforced with GFRP bars decreases with the increase of the GFRP bars ratio in the concrete section exposed to flexure bending load.

5 REFERENCES

[1] T. F. Yuan, J. Y. Lee, K. H. Min, and Y. S. Yoon, “Experimental investigation on mechanical properties of hybrid steel and polyethylene fiber-reinforced no-slump high-strength concrete,” Int. J. Polym. Sci., vol. 2019, 2019, doi: 10.1155/2019/4737384.

[2] M. A. Chowdhury, M. M. Islam, and Z. Ibna Zahid, “Finite element modeling of compressive and splitting tensile behavior of plain concrete and steel fiber reinforced concrete cylinder specimens,” Adv. Civ. Eng., vol. 2016, pp. 1–12, 2016, doi: 10.1155/2016/6579434.

[3] M. Selvakumar, S. Geetha, S. Kasturi Rangan, T. Sithrubi, and K. Sathyashriya, “Effect of glass powder as partial fine aggregate replacement on properties of basalt fibre reinforced concrete,” Mater. Today Proc., vol. 43, pp. 1460–1464, 2020, doi: 10.1016/j.matpr.2020.09.299.

[4] H. Huang, Y. Yuan, W. Zhang, R. Hao, and J. Zeng, “Bond properties between GFRP bars and hybrid fiber-reinforced concrete containing three types of artificial fibers,” Constr. Build. Mater., vol. 250, p. 118857, 2020, doi: 10.1016/j.conbuildmat.2020.118857.

[5] A. Saradar, B. Tahmouresi, E. Mohseni, and A. Shadmani, “Restrained shrinkage cracking of fiber-reinforced high-strength concrete,” Fibers, vol. 6, no. 1, 2018, doi: 10.3390/fib6010012.

[6] N. Shahrour and R. Allouzi, “Shear behavior of captive and short column effects using different basalt aggregate contents,” J. Build. Eng., vol. 32, no. October 2019, p. 101508, 2020, doi: 10.1016/j.jobe.2020.101508.

[7] A. G. Bajgirani, S. Moghadam, S. T. Tafreshi, A. Arbab, and H. Razeghi, “The Influence of Aspect Ratio of Steel Fibers on The Mechanical Properties of Concrete,” CiteSeerX, no. July, pp. 1–8, 2016.

[8] D. Y. Yoo and N. Banthia, “Mechanical properties of ultra-high-performance fiber-reinforced concrete: A review,” Cem. Concr. Compos., vol. 73, pp. 267–280, 2016, doi: 10.1016/j.cemconcomp.2016.08.001.

[9] A. Jadidi, M. Amiri, and E. Zeighami, “Experimental evaluation of steel fiber effect on mechanical properties of steel fiber-reinforced cement matrix,” Frat. ed Integrita Strutt., vol. 11, no. 42, pp. 249–262, 2017, doi: 10.3221/IGF-ESIS.42.27.

[10] A. Karimipour, M. Ghalehnovi, and J. de Brito, “Mechanical and durability properties of steel fibre-reinforced rubberised concrete,” Constr. Build. Mater., vol. 257, p. 119463, 2020, doi: 10.1016/j.conbuildmat.2020.119463.

[11] L. Jin, R. Zhang, Y. Tian, G. Dou, and X. Du, “Experimental investigation on static and dynamic mechanical properties of steel fiber reinforced ultra-high-strength concretes,” Constr. Build. Mater., vol. 178, pp. 102–111, 2018, doi: 10.1016/j.conbuildmat.2018.05.152.

[12] L. A. et. al Quresh, “Effect of mixing steel fibers and silica fume on properties of high strength concrete,” Proceedings. Int Conf. Concr. Constr. Sustain. option, pp. 173–185, 2008.

[13] Z. Li, H. Zhu, X. Zhen, C. Wen, and G. Chen, “Effects of steel fiber on the flexural behavior and ductility of concrete beams reinforced with BFRP rebars under repeated

loading," Compos. Struct., vol. 270, no. May, p. 114072, 2021, doi: 10.1016/j.compstruct.2021.114072.

[14] P. S. Song and S. Hwang, "Mechanical properties of high-strength steel fiber-reinforced concrete," Constr. Build. Mater., vol. 18, no. 9, pp. 669–673, 2004, doi: 10.1016/j.conbuildmat.2004.04.027.

[15] W. rui Yang, X. jun He, and L. Dai, "Damage behaviour of concrete beams reinforced with GFRP bars," Compos. Struct., vol. 161, pp. 173–186, 2017, doi: 10.1016/j.compstruct.2016.11.041.

[16] V. Gribniak, A. Pérez Caldentey, G. Kaklauskas, A. Rimkus, and A. Sokolov, "Effect of arrangement of tensile reinforcement on flexural stiffness and cracking," Eng. Struct., vol. 124, pp. 418–428, 2016, doi: 10.1016/j.engstruct.2016.06.026.

[17] R. Qin, A. Zhou, and D. Lau, "Effect of reinforcement ratio on the flexural performance of hybrid FRP reinforced concrete beams," Compos. Part B Eng., vol. 108, pp. 200–209, 2017, doi: 10.1016/j.compositesb.2016.09.054.

[18] A. El-Nemr, E. A. Ahmed, A. El-Safty, and B. Benmokrane, "Evaluation of the flexural strength and serviceability of concrete beams reinforced with different types of GFRP bars," Eng. Struct., vol. 173, no. June, pp. 606–619, 2018, doi: 10.1016/j.engstruct.2018.06.089.

[19] S. A. Ashour, F. F. Wafa, and M. I. Kamal, "Effect of the concrete compressive strength and tensile reinforcement ratio on the flexural behavior of fibrous concrete beams," Eng. Struct., vol. 22, no. 9, pp. 1145–1158, 2000, doi: 10.1016/S0141-0296(99)00052-8.

[20] T. P. C. for preparation of E. Code, "Egyptian Code of Practice for The Use of Fiber Reinforced Polymer (FRP) In The Construction Fields." 2005.

[21] E. O. for S. and Q. (EOS), "Part 1: Compositions, specifications and conformity criteria for common cements," vol. 1, 2009.